MATERIALS AND CONDUCTOR CONFIGURATIONS IN SUPERCONDUCTING MAGNETS*

H. Brechna
Stanford Linear Accelerator Center
Stanford University, Stanford, California

I. INTRODUCTION

The configuration, form, shape and composition of a superconducting-normal metal matrix for high energy, plasma, or solid state physics, or for other applications are primarily dictated by the performance reliability of the device to be used. Several factors do affect this, such as operational stability; electromagnetic, thermal, and mechanical stresses; manufacturing and technological problems; fatigue and environmental effects. Optimization of a composite conductor is also dictated by economic considerations.

If a superconductor is stabilized by means of adequate normal metal, and operated in the nucleate boiling region of liquid helium, the over-all current density in such a conductor is low. There are, however, possible ways to improve the over-all current density without jeopardizing operational safety in case of transient flux motion, or gross discontinuities in current or coolant supply, or other unforeseen incidents.

Flux instabilities encountered in the operation of superconducting magnets are primarily caused by power dissipation in superconductors. However, quantitative results on the instability phenomena are scarce, merely due to the circumstance that the problem is nonlinear and many material properties are not known properly.

Instability in superconductors, composite cables and conductors, and magnets has been studied by Kim and Anderson,[1] Iwasa and Williams,[2] Wipf,[3] Hart,[4] and Hancox.[5] Their qualitative observations are briefly summarized: Any high field superconductor that conforms to the Kim-Anderson model of flux release from pinning centers under the combined Lorentz force and thermal activation is intrinsically unstable. Resistance is observed in a type II superconductor when the Lorentz force exceeds the field-dependent "pinning force" determined by the defect structure of the superconductor. This "flux jump" or "flux flow" resistance yields power losses in the superconductor, which must be dissipated by the coolant in order to avoid a so-called "runaway" transition from superconductivity to normality over the entire length of the conductor.

A field or temperature disturbance changes both Lorentz (F_L) and pinning (F_p) forces, the first because of the field gradient between two points of equal magnetic field B, the second because of temperature changes due to energy dissipation. An increase in temperature reduces the pinning force. A disturbance also causes a reduction in the Lorentz force. As long as the changes $\Delta F_L > \Delta F_p$, the equilibrium is stable. On

---

*Work supported by the U.S. Atomic Energy Commission.

1. Y.B. Kim et al., Phys. Rev. 131, 2486 (1963).
2. Y. Iwasa and J.E.C. Williams, Appl. Phys. Letters 9, 391 (1966).
3. S.L. Wipf, Phys. Rev. 161, 161 (1967).
4. H.R. Hart, Jr., GE Notes (unpublished).
5. R. Hancox, Proc. IEE (London) 113, 1221 (1966).

exceeding the limit $\Delta F_L \geqq \Delta F_p$, the flux movement is accelerated until a flux jump occurs. In a magnet, instabilities are triggered by flux jumps occurring in some parts of it. When the magnetic field is increased, the field profile within the superconductor, B(r), is determined by the shielding current I_s, which flows in the conductor surface. Inside the superconductor, B is zero, except in the shielding layer of thickness $\Delta = B_{ext}/4\pi J_c$. The shielding layer has everywhere the current density J_c and is in a "critical state." As B_{ext} is increased, the front of the critical state region propagates towards the center filament of the superconductor with the velocity

$$v_L = \frac{1}{4\pi J_c} \cdot \frac{dB_{ext}}{dt} \quad . \tag{1}$$

Since the flux front is moving, an electric field is induced in the conductor according to

$$\vec{U} = \vec{v}_L \times \vec{B}_{int} \quad , \tag{2}$$

which results in a power dissipation per unit volume given by

$$P = U \cdot J_c = \frac{1}{4\pi} \cdot B_{int} \cdot \frac{dB_{ext}}{dt} \quad . \tag{3}$$

Ignoring displacement current and assuming that in the superconductor the relative permeability μ_r is unity (i.e. $B_{int} = B_{ext} = B$), the field propagation in the superconductor is given by

$$\frac{\partial B}{\partial t} = \frac{\rho}{\mu_0} \cdot \nabla^2 B = D_m \cdot \nabla^2 B \quad , \tag{4}$$

which is the magnetic diffusion equation. D_m is the magnetic diffusivity, and ρ the resistivity due to a flux disturbance in the superconductor.

For a cylindrical wire one may write Eq. (4) explicitly in the form

$$\frac{\partial^2 B}{\partial z^2} + \frac{\partial^2 B}{\partial r^2} + \frac{1}{r}\frac{\partial B}{\partial r} + \frac{1}{r^2}\frac{\partial^2 B}{\partial \varphi^2} = \frac{1}{D_m} \cdot \frac{\partial B}{\partial t} \quad . \tag{5}$$

If the magnetic field is parallel to the axis of a semi-infinite conductor, Eq. (5) is simplified to

$$\frac{\partial^2 B}{\partial r^2} + \frac{1}{r}\frac{\partial B}{\partial r} = \frac{1}{D_m} \cdot \frac{\partial B}{\partial t} \quad . \tag{6}$$

If the external magnetic field is perpendicular to the conductor axis, surface effects in a single conductor are not of great importance and thus, even in this case, solution of the diffusion Eq. (6) may yield a first order approximation and has been calculated by Wipf.[6]

Wipf[6] gives as a first approximation for the resistivity of a cylindrical superconducting wire of radius r_0 in a creeping magnetic field parallel to the conductor axis the value of

---

6. S.L. Wipf, J. Appl. Phys. 37, 1012 (1966).

$$\rho_c \cong 2.5 \times 10^{-9} \cdot \frac{r_0}{J_c} \cdot \frac{\partial B}{\partial t} \quad , \tag{7}$$

and, for the resistivity in case of a flux jump, the value

$$\rho_\Delta = 1.5 \times 10^{-10} \frac{\partial B}{\partial t} \quad . \tag{8}$$

Taking a typical value of $\partial B/\partial t = 10^3$ G/sec, we get for the case of a flux jump

$$\rho_\Delta = 1.5 \times 10^{-7} \ \Omega \cdot \text{cm} \quad ,$$

which results in a magnetic diffusivity in the superconductor of

$$D_{\Delta,m} = 12 \ \text{cm}^2 \ \text{sec}^{-1} \quad .$$

The magnetic diffusivity, D_m, is counterbalanced by the thermal diffusivity, D_{th}, of the superconductor, or generally by the thermal diffusivity of the composite conductor.

For a composite conductor consisting of a superconducting core embedded in a normal metal we may write the thermal diffusion equations:

$$\frac{\partial^2 \theta}{\partial z^2} - \frac{hf}{k_s \cdot A_s^{\frac{1}{2}}} \cdot \frac{(1 + A_n/A_s)^{\frac{1}{2}}}{1 + A_n k_n/(A_s k_s)} \cdot \theta + J_s^2 \cdot \frac{\rho_s}{k_s} \cdot \frac{1 + \rho_n A_s/(\rho_s A_n)}{1 + k_n A_n/(k_s A_s)}$$

$$= \frac{1}{D_{th,n}} \cdot \frac{D_{th,n}/D_{th,s} + A_n k_n/(A_s k_s)}{1 + A_n k_n/(A_s k_s)} \cdot \frac{\partial \theta}{\partial t} \quad , \tag{9}$$

with

$$\theta = T_c - T_b \quad ,$$

where the subscript s denotes the superconductor, n the normal shunt metal, and k, ρ, h and D are thermal conductivity, electrical resistivity, heat transfer coefficient, and thermal diffusivity, respectively. A is the cross-sectional area, and f a factor linking the over-all perimeter of the composite conductor to the cross-sectional area of the normal matrix.

Assuming that the heat flow has a velocity v_q parallel to the conductor axis and is linear, i.e.

$$\frac{\partial \theta}{\partial t} = - v_q \cdot \frac{\partial \theta}{\partial z} \quad ,$$

where v_q is the heat propagation velocity, solutions of the thermal diffusion Eq. (9) have been calculated by Stekly,[7] Whetstone,[8] Gauster et al.,[9] Lontai,[10] and Brechna.[11]

7. Z.J.J. Stekly and J.L. Zar, Avco-Everett Laboratory Report 210 (1965).
8. C.N. Whetstone and C.E. Roos, J. Appl. Phys. 36, 783 (1965).
9. L.M. Lontai, Argonne National Laboratory Engineering Notes (1966).
10. W.F. Gauster et al., Oak Ridge National Laboratory Report ORNL-T-M-2075 (1967).
11. H. Brechna, Bulletin S.E.V. (Swiss) 20, 893 (1967).

The limit of stable current is calculated from $v_q = 0$ to be:

$$I_s = \left[\frac{h \cdot \Delta T}{\rho_n} \cdot A_n S_c \right]^{\frac{1}{2}} , \tag{10}$$

where S_c is the cooled perimeter.

The two differential Eqs. (6) and (9) can be combined in a set of simultaneous nonlinear equations, and we may conclude, for a purely adiabatic representation, that no instability occurs unless

$$\left. \frac{\Delta Q_m}{\Delta T} \right|_{T_1} \geqq \left. \frac{\Delta Q_{th}}{\Delta T} \right|_{T_1}$$

or, in simplified form, unless $D_m \geqq D_{th}$. ΔQ_m = magnetic energy difference, and ΔQ_{th} = thermal energy difference.

Referring now to Table I, the thermal and magnetic diffusivities of a number of materials are presented at 4.2°K. Data for thermal diffusivities as a function of temperature are given in Fig. 4.

At $T \leqq T_c$ the thermal diffusivities of type II superconductors are small compared to the magnetic diffusivities, and thus we may conclude that during a flux jump, which has a duration of only a few microseconds, the superconductor may be thermally isolated from the substrate. Due to the poor thermal conductivity in the superconductor, the temperature distribution inside the superconductor is anisotropic, and thus the exact evaluation of the diffusion mechanism proves to be difficult and will be treated later.

In a composite conductor we have three regions of flux exclusions:

a) Field stability: If the field or current perturbance has subsided, the conductor recovers its superconducting state.

b) Metastability or limited instability: A small perturbance may drive the conductor normal, but the region of normality may subside when the conductor transport current is reduced below its recovery value.

c) Runaway instability: Region of normality may propagate over the entire length of the conductor.

Field stability ($d\varphi/dt$ and $d\rho/dt$ must be limited) is achieved by adding normal metal to the superconductor. In this case the bond between superconductor and normal metal must be appropriate (thermoelectrical bond) in order that the boundary layer shall not decelerate the heat transfer from the superconductor to the normal metal.

The temperature rise due to $d\rho/dt$ is limited by utilizing materials of high thermal capacity such as silver, lead, or helium within a composite conductor.

The solution of Eqs. (6) and (9) suggests that the heat capacity ($c_p \delta$) of the system must be improved. Based on one-dimensional models, Hancox[12] gives the upper stable screening field

$$H_s \leqq (8\pi \, c_p \delta \cdot T_0)^{\frac{1}{2}} . \tag{11}$$

---

12. R. Hancox, Phys. Letters 16, 208 (1965).

TABLE I

Properties of Elements and Alloys at 4.2°K

Material	Density (g/cm^3)	Specific Heat ($J/g\ ^oK$)	Thermal Capacity ($J/cm^3\ ^oK$)	Therm. Conductivity ($W/cm\ ^oK$)	Therm. Diffusivity (cm^2/S)	Magnetic[a] Diffusivity (cm^2/S)
Ag (99.999%)	10.6	1.35×10^{-4}	14.3×10^{-4}	130	9.0×10^{4}	0.08
Al (99.996%)	2.7	2.8×10^{-4}	7.56×10^{-4}	33	4.36×10^{4}	1.25
Cu (99.95% an)	8.95	10^{-4}	8.95×10^{-4}	2.5	0.28×10^{4}	0.95
In (99.993%)	7.28	1.2×10^{-3}	8.73×10^{-3}	8.5	0.973×10^{4}	2.47
Na (99.999%)	1.009	1.7×10^{-3}	1.71×10^{-3}	48	28.07×10^{4}	0.135
Pb (99.998%)	11.25	8.0×10^{-4}	90.0×10^{-4}	22	0.24×10^{4}	0.32[b]
He	15×10^{-3} @ 15 atm	2.1 @ 15 atm	31.5×10^{-3} @ 15 atm	3.14×10^{-4}	10^{-2}	
Nb_3Sn	5.4[c]	2.1×10^{-4}	11.34×10^{-4}	4.0×10^{-4}	0.35	
Nb25%Zr	8.1	1.8×10^{-4}	14.58×10^{-4}	0.8×10^{-3}	5.4	
Nb60%Ti	5.6	1.8×10^{-4}	10.1×10^{-4}	1.2×10^{-3}	1.18	

[a] Data for resistivity without strain.

[b] $H > H_c$.

[c] The density of Nb_3Sn is about 8 g/cm^3, but the c_p calculation from Vieland's measurements (Ref. 20) indicate $\delta = 5.4\ g/cm^3$.

Depending on the diameter ratio of the superconductor to normal metal d_s/d_n, the average stable current density in the composite conductor is given by

$$J_{av} = \frac{1}{d_n}\left[\frac{3 \times 10^9}{4\pi} c_p \delta \cdot \frac{d_s}{d_n} \cdot T_0\right]^{\frac{1}{2}} . \qquad (12)$$

T_0 is a temperature less than the critical temperature of the superconductor; $[T_0 = - J_c/(dJ_c/dT)]$.

The diameter of a single superconductor filament must follow the relation:

$$d_f \leqq \frac{1}{J_c}\left(\frac{3 \times 10^9}{4\pi} c_p \delta \cdot T_0\right)^{\frac{1}{2}} \qquad (13)$$

to avoid flux jumps.

The balance between the magnetic and thermal diffusivity also suggests improving the ratio between the perimeter and cross-sectional area of individual superconductors, which leads to a conductor with many filamentary superconductors. The minimum size and the distribution of individual superconducting filaments in the normal metal substrate and the quality of the surface bond are presently being investigated by several laboratories. However, it may be pointed out that the heat dissipated by a disturbance in individual filaments must be absorbed and conducted to the coolant bath, before it may heat up the superconductor such that the region of normality can spread over the entire length of the composite conductor.

In a composite conductor the distribution of filaments in the matrix leads to inductive coupling of magnetization currents which can lead, in turn, to heating of the conductor during flux change (charging or discharging rate sensitivity) and may trigger flux jumps. The normal metal substrate must have adequate thermal capacity to absorb this additional heating phenomenon.

Improvement of the heat transfer coefficient by utilizing forced cooling with helium was proposed by Brechna[13] using hollow (internally cooled) composite conductor. Using supercritical helium was suggested by Kolm.[14] With this scheme, using a particular conductor geometry (over-all dimensions 0.5 x 0.5 cm, coolant passage 0.22 x 0.22 cm) and a flow rate of 0.8 liter/min of helium, a stable current density of 1.6×10^4 A/cm^2 was measured at an external field of 5 T.

Introducing of liquid or gaseous helium in the composite matrix (porous substrate) by using sintered porous metals of low sintering temperature such as cadmium has been proposed by Brechna and Garwin.[15] The substrate porosity can be 50% or less. Individual, partially stabilized, superconducting filaments are located within the porous substrate, which acts as a support structure and enables the coolant to be in contact with the filaments. Although data of over-all current densities of such conductors are not available at present, calorimetric measurements indicate that an over-all thermal capacity of $\sim$ 0.15 J/cm^3 $^\circ$K can be achieved with porous copper immersed in liquid helium.

---

13. H. Brechna, in Proc. Intern. Cryogenic Engineering Conf., Kyoto, 1967, p. 119.
14. H.H. Kolm, in Proc. Intern. Symp. Magnet Technology, Stanford, 1965, p. 611.
15. H. Brechna and E. Garwin, SLAC Proposal 1967.

Smith et al.[16] suggests the use of fine filaments embedded in a high resistance matrix (i.e., Cu-Ni alloy), in order to reduce cross magnetization currents between extreme located filaments in the matrix. The diameter of individual superconductor filaments should not exceed 5×10^{-3} cm. They also propose to twist the bundle of filaments in the matrix with a periodicity of about 2-3 cm.

Improvement of over-all current densities in the magnet shall by no means affect the safety of the magnet. High current densities at transverse high flux densities in large magnets will yield Lorentz forces which make the use of conductor reinforcement imperative. Additional stresses are produced by the differential contraction of various materials. Thus in large magnets the stress and strain behavior of the conductor and insulation material will primarily dictate the over-all current densities, not the instability phenomena. Table II illustrates the over-all current densities and conductor stresses in some procured and proposed high energy magnets.

One more factor which dictates the form and composition, as well as coil configuration and reinforcement, is the field reproducibility. Magnets generally are warmed up in periods between experiments. Fatigue behavior is encountered in insulation structures and in highly stressed substrates. Coils may become loose and flux jumps due to wire movements may occur.

It is evident that average current densities in coils are not primarily dictated by the ac behavior of the superconductor alloys, but by the stress-strain properties of the composite. Large magnets ($E_{field} > 1$ MJ) will be designed with moderate average current densities, up to 15×10^3 A/cm^2, while smaller coils may achieve current densities in excess of 5×10^4 A/cm^2 at fields of 4 T.

It is important that the maximum stress on the composite conductor shall not exceed $\sim$ 20% of the 4.2°K yield strength in order to avoid early fatigue.

Prior to a discussion of optimization studies, the physical and mechanical properties of composite conductors are presented in quantitative form.

II. PHYSICAL AND MECHANICAL PROPERTIES OF SUPERCONDUCTORS TYPE II, NORMAL METALS, AND COMPOSITE CONDUCTORS

1. Thermal Conductivity

The thermal conductivities of Nb(25%)Zr wires and bars[11] at $B_{ext} = 0$ and $B_{ext} = 5$ T are illustrated in Fig. 1 and compared to data for Nb(60%)Ti wires at $B_{ext} = 0$ measured at MIT-NML,[17] and data for Nb_3Sn measured by Cody.[18] In Nb(25%)Zr the conductivity values are different for 0.025 cm wires in the longitudinal direction and for bars, which suggests that the superconductor is thermally anisotropic. The effect of magnetic field is also pronounced in all superconducting type II alloys.

It may be pointed out that the major contribution to the thermal conductivity at temperatures below transition values is from phonons rather than electrons, which become less active. Wiedemann-Franz law in the usual form is not applicable to superconductors and to commercially available normal metals used with superconductors.

---

16. P.F. Smith et al., Brit. J. Appl. Phys. 16, 947 (1965).
17. J.R. Hale, MIT Bitter National Magnet Laboratory, private communication (1968).
18. G.D. Cody and R.W. Cohen, Rev. Mod. Phys. 36, 121 (1964).

2. Electrical Resistivity

The electrical resistivities of three types of superconductor type II are given in Fig. 2. Measurements have been performed at low external field. Further investigations at various external fields are in progress. The electrical resistivities of some normal materials are compared to the data for superconductors. For OFHC copper the electrical resistivity as a function of external field is shown in Fig. 3. The resistivity follows the correlation[19]:

$$\rho_{4.2^oK,B} = \rho_{300^oK,B=0}\left[\frac{0.9}{\rho_{300^oK,B=0}/\rho_{4.2^oK,B=0}} + 0.25 \times B \times 10^{-2}\right] , \qquad (14)$$

where B has the dimension of (T).

3. Thermal Diffusivity

The thermal diffusivities of several normal metals are illustrated in Fig. 4. Data at 4.2°K for some superconductors type II are given in Table I.

4. Specific Heat

Specific heats and thermal capacities of metals and a few superconductors type II are given in Table I. The specific heats for Nb(25%)Zr and Nb_3Sn are illustrated in Fig. 5 and may be compared to values given for some normal metals.[20] Data for NbTi are presently not available.

5. Mechanical Properties

The effect of cold work (tension on the composite conductor) on resistivity was measured by Brookhaven,[21] and RHEL.[22] Extensive data on the effect of stress on elongation of copper and aluminum are obtainable from NBS handbooks. The effect of stress on resistivity and cold work on composite conductors (NbTi thermoelectrically bonded to OFHC copper) is illustrated in Figs. 6a and 6b.

From these measurements one obtains a Poisson ratio at 4.2°K of m = 0.32 and a modulus of elasticity of E = (1.7-1.8) $\times 10^6$ kg/cm^2 according to the type of composite, compared to m = 0.33 and E = 1.34 $\times 10^6$ kg/cm^2 for OFHC copper.

The modulus of elasticity of NbTi alloy depends grossly on the Ti content.

III. COMPOSITE CONDUCTORS AND CABLES

The size and shape of the composite conductor, the ratio of superconductor to normal metal, the quality of the metallurgical (thermoelectrical) bond between superconductor and normal metal, the thermal capacity of the system, and the heat transfer from superconductor to the coolant are directly related to the stable current density

---

19. C.W. Whetstone et al., in Proc. Intern. Cryogenic Engineering Conference, Kyoto, 1967, Paper B7.
20. L.J. Vieland and A.W. Wicklund, Phys. Letters 23, 227 (1966).
21. Bubble Chamber Group, Brookhaven National Laboratory Report BNL 10700, p. 78 (1966).
22. P. Clee, Rutherford High Energy Laboratory Report EDN 0001.

limit of the composite conductor. As mentioned, stability against flux motion (jumps) is presently achieved by using relatively large cross sections of normal metals surrounding individual superconducting filaments, providing adequate coolant channels for circulating helium, insuring direct contact of coolant to the normal metal or superconductor, subdividing the superconductor in small filamentary wires adequately spaced in the normal metal matrix, and enhancing the thermal capacity of the conductor.

The conductor is stable up to the critical current of the superconductor and even at currents somewhat higher, with the excess current flowing through the normal metal.

Magnets are generally exposed to thermal and magnetomechanical stresses. In many applications, even if average high current densities with regard to flux instabilities would be permissible, material stress-strain behavior would limit the upper over-all current density limit.

Several design problems must be considered prior to the choice of current density field parameters. Among these are questions relating to:

a) Over-all field or field-gradient distribution in a usable volume.

b) Field or gradient reproducibility over the lifetime of the experimental setup.

Generally, field uniformity in the order of 10^{-4} and field reproducibility in the order of 10^{-5} are required in large multimegajoule experimental magnets and in beam transport magnets.

These problems have been one factor limiting the current densities in medium size and large superconducting magnets to less than 5000 A/cm^2. With the reinforcement technology and better understanding of the flux instability phenomena, it is now possible to design magnets with over-all current densities of 1.5×10^4 A/cm^2 at fields of 5 T. Table II illustrates a few examples of tested, procured, and proposed experimental magnets with field energies in excess of 1 MJ.

From an earlier stage of partially or completely stabilized superconducting cables (roped superconducting and copper filaments) impregnated with indium, or for strength purposes with silver-tin alloys (Fig. 7), the technology of producing long conductors has been advanced considerably. Modern composite conductors contain several hundred superconducting filaments, metallurgically bonded to a copper or aluminum matrix (Fig. 8). While in a cable, due to manufacturing difficulties, individual superconductors had seldom a diameter as small as 10^{-2} cm, in composite conductors, individual filaments of NbTi may have diameters of 5×10^{-3} cm or less.

Flux jump instabilities are present in all superconducting magnet wires, when the diameter of the individual filament is larger than the value calculated from (12). However, larger filament sizes may be usable, if the region of normality can be cooled prior to propagation of heat along the conductor. Partially stable or metastable conductors are interesting for dc applications if adequate cooling is provided. A one-dimensional solution of Eqs. (15) and (9), or systematic measurements of flux jump instabilities in various conductor configurations can result in an adequate lower limit of filament diameter and a ratio of normal metal to superconductor.

Measurements with small size coils (a_1 = 2-4 cm; a_2 = 10 cm; 2b = 15 cm, field energies $\leqq$ 50 kJ, maximum field 6.5 T) built by partially stabilizing six-stranded Nb(60%)Ti cables of the type shown in Fig. 7 with copper, and insulated according to Fig. 8 show an interesting flux jump pattern. At self-fields smaller or equal to H_{c1}, no flux jumps were measured (Fig. 9). By increasing the transport current and with it the field at a constant rate (dB/dt = const), flux jumps were made to occur suddenly,

TABLE II

Procured, Designed, and Proposed Large Superconducting Magnets

Laboratory	Type	i.d. (cm)	o.d. (cm)	Length (cm)	$B_{0,0}$ (T)	B_m (T)	J_c A/cm^2	$\lambda J_{over-all}$ A/cm^2	σ_{hoop} kg/cm^2	Remarks
1. Procured and tested magnets										
Avco	Saddle	30.5	84	305[a]	3.7	4.25	1.4×10^5	$< 10^3$	?	Nb(25%)Zr Cu-Strip. Cond.
CERN	Helmholtz	40	66.5	66	6	6.6	6×10^4	5×10^3	1.4×10^3	Nb, Ti and Cu Cond. Nb, Ti and Al Cond.
NASA	Solenoid	15	48.5	34.5	13.5	13.8	2.45×10^5	1.34×10^4	2.16×10^3	Nb_3Sn and Hastelloy-Cu Stabilized Cond.
SLAC	Helmholtz	30	90	70	7	8	3.7×10^4	4×10^3	10^3	Nb, Ti and Cu Cable
2. Procured magnets										
Argonne N.L.	Helmholtz (B.B.C.)	488	550	287	2	2	4.0×10^5	10^3	7.62×10^2	Nb, Ti and Cu Composite Strip
Brookhaven N.L.	Helmholtz (B.B.C.)	240	276	224	3	4	1.8×10^5	2.53×10^3	6.4×10^2	Nb, Ti and Cu Comp. Strip, SS Reinforced
3. Proposed magnets										
Brookhaven N.L.	Helmholtz (B.B.C.)	498	589	430	3	4.05	1.75×10^5	1.1×10^3	1.13×10^3	Nb, Ti and Cu Comp. Strip, SS Reinforced, with $\sigma_h = 3 \times 10^3 kg/cm^2$
Rutherford H.E.L.	Helmholtz (B.B.C.)	190	340	230	7	8	3.7×10^4	1.2×10^3	10^3	Nb, Ti and Cu Comp. Strip, SS Reinforced
SLAC	Helmholtz (B.B.C.)	140	236	130	7	8.2	3.0×10^4	2.5×10^3	10^3	Nb, Ti and Cu hollow Composite Cond. with SS reinforcement with $\sigma_h = 3.2 \times 10^3 kg/cm^2$
NAC	Helmholtz	710	880	426.5	3.8	6.0	8.0×10^4	1.4×10^3	1.06×10^3	Nb, Ti and Cu hollow Composite Cond., SS reinforcement, with $\sigma_h = 3.8 \times 10^3$ kg/cm^2

[a] The uniform field length is approximately 80 cm.

and they repeated themselves at regular time intervals. When central fields of ~ 1.5 T were reached, corresponding to about 1.9 - 2 T at the conductor, the intervals between flux jumps became shorter until no more, with the exception of a few sporadic ones, were observed. The number of total flux jumps over a particular field region remained constant regardless of the speed of flux sweep. However, at very low dB/dt values, only a few flux jumps were observed (Fig. 10). This flux jump behavior is observed with increasing and decreasing fields.

The occurrences of the flux jumps can be referred to conductor movements in the coil due to the Lorentz forces. The spiral-wound insulation (Nomex) is gradually compressed. If a few interturn and interlayer short circuits were originally present, the inductance in the conductor region changes in jumps because of the enhancement of the local short circuits, leading to flux jumps. When the coils are compacted due to the magnetic forces, no wire movements are encountered and flux jumps disappear. However, in this region, where flux jumps due to short circuits are generated, flux jumps due to the flux motion may occur also, until the flux has penetrated to the central fibers of the individual filaments. When wire movement and internal short circuits were prevented, no flux jumps due to change in transport current were observed. Flux jumps did occur sporadically when the external field was altered.

Critical current densities were reached in several types of composite conductors (Fig. 11), where the diameters of individual filaments were ~ 1.5×10^{-2} cm and the copper-to-superconductor ratio exceeded 3:1. For most designs, if appropriate cooling can be provided, a copper-to-superconductor ratio of 3:1 is adequate. Filament diameters of 10^{-2} cm may be the lower limit for most dc magnets, operating at fields up to 8 T.

Single layer coils with an inner diameter of $2a_1 = 5$ cm were placed inside a 7 T superconducting magnet, and thermal and magnetic pulses, as proposed by Iwasa and Williams,[23] were applied to the conductor to measure the minimum propagating current density (J_{mp}), and the quenching (J_c) and recovery (J_R) current densities.

With conductors up to sizes of 0.4×0.4 cm^2, and numbers of filaments up to 78 with Nb(60%)Ti filament diameters up to 25×10^{-2} cm, the following minimum propagating currents were measured:

$$B = (B_{ex} + B_{self}) = 7 \text{ T} : J_{mp} \cong 10^4 \text{ A/cm}^2$$

$$B = 6.3 \text{ T} : J_{mp} \cong 1.3 \times 10^4 \text{ A/cm}^2 .$$

Approximately 70% of the cooling surface area was exposed to helium. Surface heat flux measured at 7 T and $J_{mp} = 10^4$ A/cm^2 was $h\Delta T = 0.76$ W/cm^2.

For high field magnets, where magnetomechanical stresses on the composite conductor may exceed the elastic limit of the composite conductor, reinforcements based on stainless steel, or Be(2.5%)Cu strips, films, or wires are used for reinforcement. In order to avoid material creep due to repeated thermal contraction and expansion (thermal cycling in repeated operations), the maximum hoop stress on the conductor shall not exceed certain limits below the yield strength of the material. Figure 12 shows a possible type of reinforced composite conductor where stainless steel wires are inserted in the copper matrix.

---

23. Y. Iwasa and J.E.C. Williams, J. Appl. Phys. 39, 2547 (1968).

Stress-strain studies by the H_2 bubble chamber group at RHEL[24] indicate that hard copper, annealed and tempered, yields a higher strength ($\sim$ 6%) and a smaller resistivity increase ($\sim$ 20%) at 0.1% strain than copper directly work-hardened (1/8 hard) from soft annealed copper.

Similar methods of reinforcing Nb_3Sn ribbon by means of stainless steel or Hastelloy substrates have been utilized in high current density pancake type wound magnets. In these cases the substrate will carry practically all the thermal and magnetomechanical load.

IV. HOLLOW COMPOSITE CONDUCTORS

First tests with hollow composite conductors date back to November 1965.[25] Short-sample tests on square hollow conductors of 0.63 x 0.63 cm^2 over-all dimensions with a coolant hole of 0.3 x 0.3 cm^2 were carried out. Nb_3Sn strips were indium-soldered in two grooves on the outside surfaces. The ratio of Cu to superconductor was approximately 20:1. Saturated liquid helium passing at a speed of $\sim$ 25 cm/sec was passed through the hole. Although average current densities measured were less than 10^3 A/cm^2 at $\sim$ 4 T, the results were encouraging and justified further studies.

With the same conductor configuration, a one-layer solenoid with an i.d. of 15 cm and 8 turns was built and placed inside the 30 cm coil for evaluation of transport current density vs helium flow rate. Short-sample behavior could be repeated although no supercritical helium was utilized. Figures 13 and 14 illustrate at 4 T external field, the current-voltage characteristics of the coil with flow rates of saturated liquid helium as the parameter. At a helium speed of 87 cm/sec, and an external field of 4 T, an average current density of 2.8 x 10^3 A/cm^2 was measured, which complies with the Nb_3Sn short-sample critical current.

In the meantime, hollow superconductors using copper shunt metal and Nb(60%)Ti are commercially available. Figures 15 and 16 illustrate two such conductors where, in the case of 0.5 x 0.5 cm^2 conductor with a coolant hole of 0.22 x 0.22 cm^2, the copper-to-superconductor ratio is 2.8:1. The cross sections of the superconducting filaments were severely deformed during the first trial manufacturing. Sweeping the current at various speeds up to 4000 A, which is the limit of the laboratory capability, did not cause any detectable flux jumps ($dI/dt > 4000$ A/sec), nor did introduction of heat pulses of 100 J quench the conductor.

To correlate the results obtained from square composite conductors, tests on long hollow superconductors having a copper-to-superconductor ratio of 4:1 - 5:1 and superconductor filament sizes of $\sim$ 0.025 cm diameter are being prepared. The composite hollow conductor will be wound in pancakes or double pancakes and the conductor will be insulated by means of glass fiber tapes impregnated with filled epoxies, to match thermal contraction.

The main advantage of hollow conductors is in reliable performance, the coils are compact, and support problems are easy to solve. The helium reservoir is omitted. The coil is embedded in superinsulation and placed in a vacuum vessel. A possible method of insulating individual hydraulic passages by means of reinforced ceramic tubing is shown in Fig. 17.

---

24. D. Thomas, Rutherford High Energy Laboratory, private communication.

25. H. Brechna, Argonne National Laboratory Report 7192, p. 29 (1966).

A few measured and calculated properties of hollow superconductors follow:

1. Anisotropy Effects

For hollow conductors, as well as for other composite conductors, anisotropy effects are of prime importance. The critical current density in strip shaped composite conductors has varied in some cases to about 5:1 when placed parallel and perpendicular to the magnetic field. The anisotropy effect has been measured also in composite conductors where the individual superconducting filaments were not distorted. For hollow composite conductors the anisotropy effect is less pronounced, as seen from Fig. 18. A distortion of the filaments in the copper or aluminum matrix is with the present technologies unavoidable; it is proposed to twist or transpose the superconducting filaments in the matrix, reduce the filament size to $\sim 1.5 \times 10^{-2}$ cm, and avoid filament distortion by more than an aspect ratio of 2:1.

2. Minimum Heat Flux

In large magnets using pool boiling, stable heat flux values have seldom exceeded 0.4 W/cm^2 (well within nucleate boiling region of saturated liquid helium).

The minimum heat flux value is calculated from the relation[26]

$$h\Delta T_{min} = 0.5 \left[T_V \cdot \delta_V\right] \left[\frac{10^{-5} \cdot \sigma(\delta_L - \delta_V)}{(\delta_L + \delta_V)^2}\right]^{0.25}, \qquad (15)$$

where T_V = heat of vaporization (J/g),

$\delta_V; \delta_L$ = densities of vapor and liquid (g/cm^3),

σ = liquid surface tension (N/cm).

The main heat flux is not a function of the hydraulic diameter, d_h, of the coolant flange, when $d_h \geqq 0.04$ cm. However, a pressure drop dependency is observed. At a pressure drop of $\Delta p = 1$ kg/cm^2 we calculate $h\Delta T_{min} = 0.18$ W/cm^2, which corresponds to measurements by Wilson.[27]

For forced cooling, utilizing supercritical helium at pressures > 2.3 kg/cm^2, the heat transfer coefficient is given by the well-known correlation:

$$h = C \cdot \frac{k_f}{d_h} \cdot (Re)_f^{0.8} \cdot (Pr)_f^{0.4} \qquad (16)$$

with

$$Re = \frac{d_h \cdot \delta \cdot v}{\eta} = \text{Reynolds number},$$

and

$$Pr = \frac{C_p \eta}{k} = \text{Prandtl number}.$$

---

26. M.A. Green, University of California, Lawrence Radiation Laboratory Engineering Note UCID 3050 (1967).

27. M.N. Wilson, Rutherford High Energy Laboratory, private communication (1966).

The Nusselt number coefficient C has values in the range 2.3×10^{-2} to 4×10^{-2}, and in the above expressions

v	= mean helium velocity	(cm/s)
η	= viscosity	(g/cm·s)
C_p	= specific heat	(J/g ^oK)
k	= thermal conductivity	(W/cm·^oK)

Unfortunately, quantitative data for η and k of supercritical helium are available only in limited pressure and temperature intervals. Detailed data are currently being measured by NBS.[28]

For supercritical helium at 15 kg/cm^2 passing through a channel of $d_h = 0.5$ cm with a speed of $v = 5$ m/sec, we obtain for $T \cong 4.5^oK$:

$$h = 0.516 \text{ W/cm}^2\ ^oK \ ,$$

using the lower limit for $C = 2.3 \times 10^{-2}$.

Allowing only a temperature rise of 2^oK in the liquid, a heat flux of

$$h\Delta T = 1.03 \text{ W/cm}^2$$

may be carried by the supercritical helium.

If a certain length of the hollow superconductor is driven normal, the heat propagates along the composite conductor as well as along the coolant, which, in turn, will warm up the downstream portion of the conductor. We define a length of normality as "critical" when the region does not propagate along the total length of the conductor. Any length of normality shorter than the critical length is "self-healing" and the normal region will disappear. If the normal region is longer than the critical length, it may spread along the conductor and lead to a coil quench.

For a hollow (inner cooled) composite conductor, the thermal diffusivity Eq. (9) must be extended by the heat equation in the moving coolant. For one-dimensional heat flow along the conductor we may write:

$$\frac{d^2\theta}{dz^2} - \frac{hf}{k_s A_s^{\frac{1}{2}}} \cdot \frac{(1 + A_n/A_s)^{\frac{1}{2}}}{1 + A_n k_n/(A_s k_s)} \cdot (\theta - \theta_f) + J_s^2 \cdot \frac{\rho_s}{k_s} \cdot \frac{1 + \rho_n A_n/(\rho_s A_s)}{1 + k_n A_n/(k_s A_s)}$$

$$+ v_{q_c} \cdot \frac{1}{D_{th,n}} \frac{D_{th,n}/D_{th,s} + A_n k_n/(A_s k_s)}{1 + A_n k_n/(A_s k_s)} \frac{d\theta}{dz} = 0 \qquad (17)$$

$$k_f A_f \frac{d^2\theta}{dz^2} + c_{p,f} \delta_f v_f \cdot \frac{\partial\theta}{\partial z} + c_{p,f} \delta_f \frac{\partial\theta}{\partial t} + hf\, A_f(\theta - \theta_f) = 0 \ . \qquad (18)$$

---

28. NBS Proposal, 1967.

where $c_{p,f}$ = specific heat of the fluid,

v_f = velocity of the fluid,

v_{q_c} = propagation velocity of the normal region,

with $$\theta = T_c - T_b \quad .$$

A set of three simultaneous equations, including magnetic diffusivity Eq. (4), must be solved to give conditions for a flux jump or a quasi steady state behavior.

3. Pressure Drop

For a single phase flow through a hydraulic passage the pressure drop may be given by

$$\Delta p = \delta \cdot \frac{v^2}{2g} \left[2C_f \frac{\ell}{d_h} + (C_e + C_c) \right] \quad ; \tag{19}$$

where C_f = friction coefficient,

C_c = contraction factor at the passage entrance,

C_e = expansion factor at the passage exit.

The entropy-enthalpy diagram for supercritical helium indicates that a pressure drop along a hydraulic passage for a constant (J/g) is associated with a temperature rise along the passage. A pressure drop of $\Delta p = 5$ kg/cm^2 will yield a temperature rise in the supercritical helium of $\sim 0.8^{\circ}$K. This rise in coolant temperature is undesirable in high field magnets ($B_{0,0} \geq 7$ T) because of the considerable reduction in J_c.

A possible scheme is to operate with high pressure drops and consequently high coolant velocities only during magnet charging. In steady-state conditions, the pressure drop can be reduced to operate with helium velocities of ~ 1 m/sec. The refrigerator system will operate during this time at a fraction of its nominal cooling power.

4. Frictional Losses

Supercritical helium passing at a certain speed through a hydraulic passage will generate frictional losses at the interface on the passage walls. The losses can be calculated from shearing stresses on the helium boundary layer[29]:

$$\tau_0 = \frac{1}{8} \cdot \lambda \cdot \frac{\delta}{g} \cdot \bar{v}^2 \quad . \tag{20}$$

λ is the frictional resistance coefficient, explicitly written as:

$$\lambda = 0.3164 \left(\frac{\bar{v} \cdot \delta \cdot d_h}{\nu} \right)^{-\frac{1}{4}} \quad , \tag{21}$$

where ν is the dynamic viscosity.

---

29. J. Kestin, Boundary Layer Theory (McGraw-Hill, 1960), 4th ed.

Inserting λ in Eq. (20) we get:

$$\tau_0 = 3.955 \times 10^{-2} \frac{\delta_f}{g} \cdot \bar{v}^{7/4} \cdot \nu^{\frac{1}{4}} \cdot d_h^{-\frac{1}{4}} \quad . \tag{22}$$

τ_0 changes with $\bar{v}^{7/4}$ rather than linearly, as for laminar flows, according to Stokes' law.

The frictional losses per unit surface area are given by:

$$P = \tau_0 \cdot \bar{v}$$
$$= 3.955 \times 10^{-2} \cdot \frac{\delta}{g} \cdot \bar{v}^{11/4} \cdot \nu^{\frac{1}{4}} \cdot d_h^{-\frac{1}{4}} \quad . \tag{23}$$

Hydraulic passages in large magnets have generally a length of $\sim$ 100 m and many passages may be connected in parallel, hydraulically but in series electrically. The choice of pressure drop, helium velocity, and obtainable heat flux should be correlated such that frictional losses do not exceed 10% of the total static losses.

CONCLUSIONS

To optimize size, geometry and type of a composite superconductor, one has to consider the following requirements:

1) Field distribution within the useful aperture of a magnet.
2) Field reproducibility over the operational lifetime of the equipment.
3) Operational reliability.
4) Economy of operation.

With the type of magnet to be designed, the basic field and force distributions over the coil are known, which automatically provide a first order estimate for the over-all dimensions of the conductor and the necessity for reinforcements.

Instabilities due to flux motion on the other hand dictate the size of individual films or filaments, their distribution, the choice of substrate, the enthalpy of the system, and cooling methods.

It is evident that small size magnets, where Lorentz forces on the conductor are not of prime importance, can be built on the basis of Nb_3Sn films on a Hastelloy substrate and stabilized by means of copper, silver, or superfluid helium. Over-all metastable current densities achieved in such magnets may exceed 5×10^4 A/cm^2 at transverse fields of 5 T.

Although only edge cooling has been widely used, new ways of cooling flat conductor surface are sought.

For large magnets, where Lorentz forces become dominant, moderate over-all current densities in the order of 1.5×10^4 A/cm^2 at 5 T may be feasible if the diameter of individual filaments in the substrate is such as to comply with Eq. (13). For ac applications flux jumps must be avoided entirely, which indicates that individual filament size should be $\sim 3 \times 10^{-3}$ cm. For dc application and efficient cooling, a filament diameter of 1.5×10^{-2} is adequate where the copper-to-superconductor ratio may be 3:1. The diameter of individual superconductors for ac application is typically of a size given by the relation $d_f \cdot J_c \leqq 1500$ A/cm. For most dc applications with

improved matrix heat capacity, this relation is conservative and can be at least doubled. The thermal capacity of the system can be improved considerably if supercritical helium is passed through the coolant passage of a porous matrix supporting individual, partially stabilized superconductors. A conductor in this form is not only useful for dc magnet application, but also for ac magnets and power transmission. The porous matrix may be sintered cadmium with a porosity of 50% or more to allow helium gas to be in direct contact with the superconductor. Its sole purpose is to support individual superconducting filaments and hold them in place along the hollow conductor. For dc applications, composite conductors based on a copper matrix and filamentary NbTi wires are widely used.

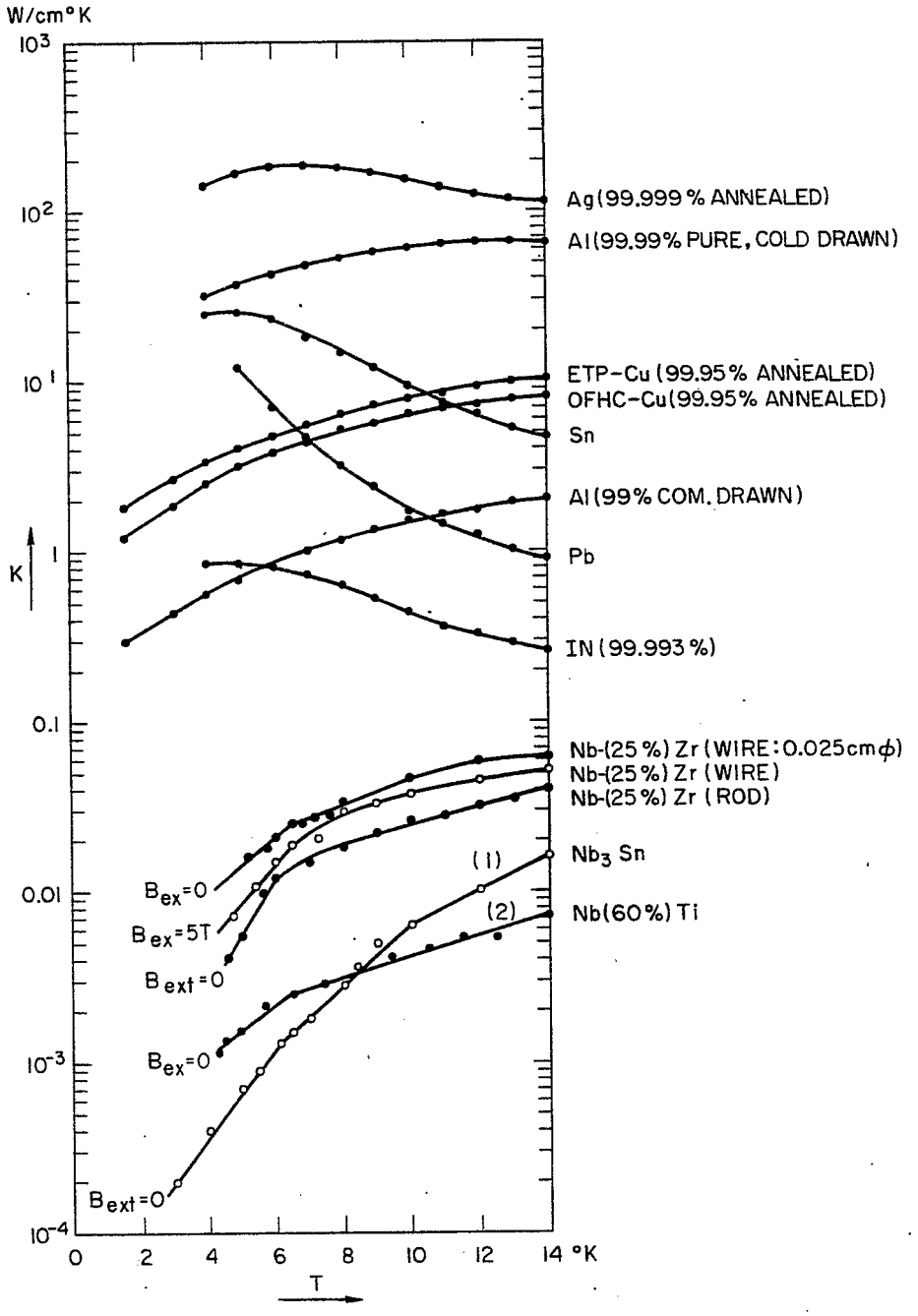

Fig. 1. Thermal conductivities of superconductors type II and normal metals.
(1) From Reference 18.
(2) From Reference 17.

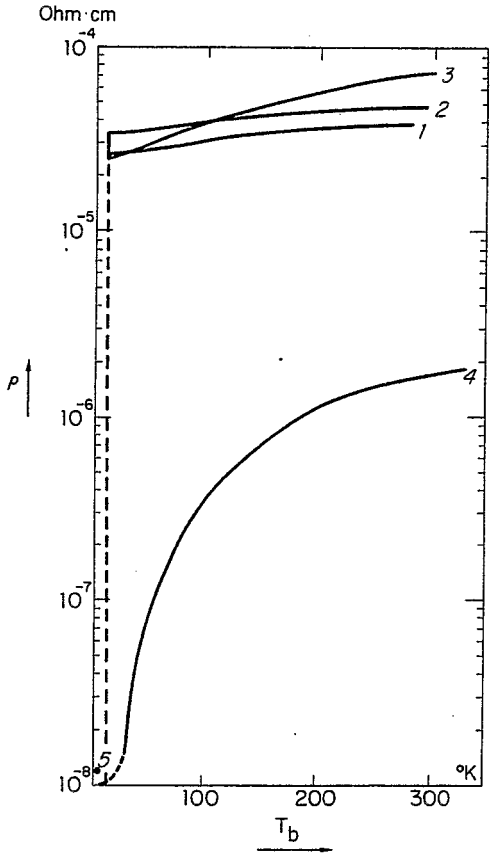

Fig. 2. Electrical resistivities of superconducting type II materials.

1. Nb_3Sn.
2. Nb(25%)Zr.
3. Nb(60%)Ti.
4. 99.999% pure annealed copper.
5. 99.995% OFHC copper as received, not annealed, $\rho_{4.2^\circ K, B=0} = 1.2 \times 10^{-8}\ \Omega\cdot cm$.

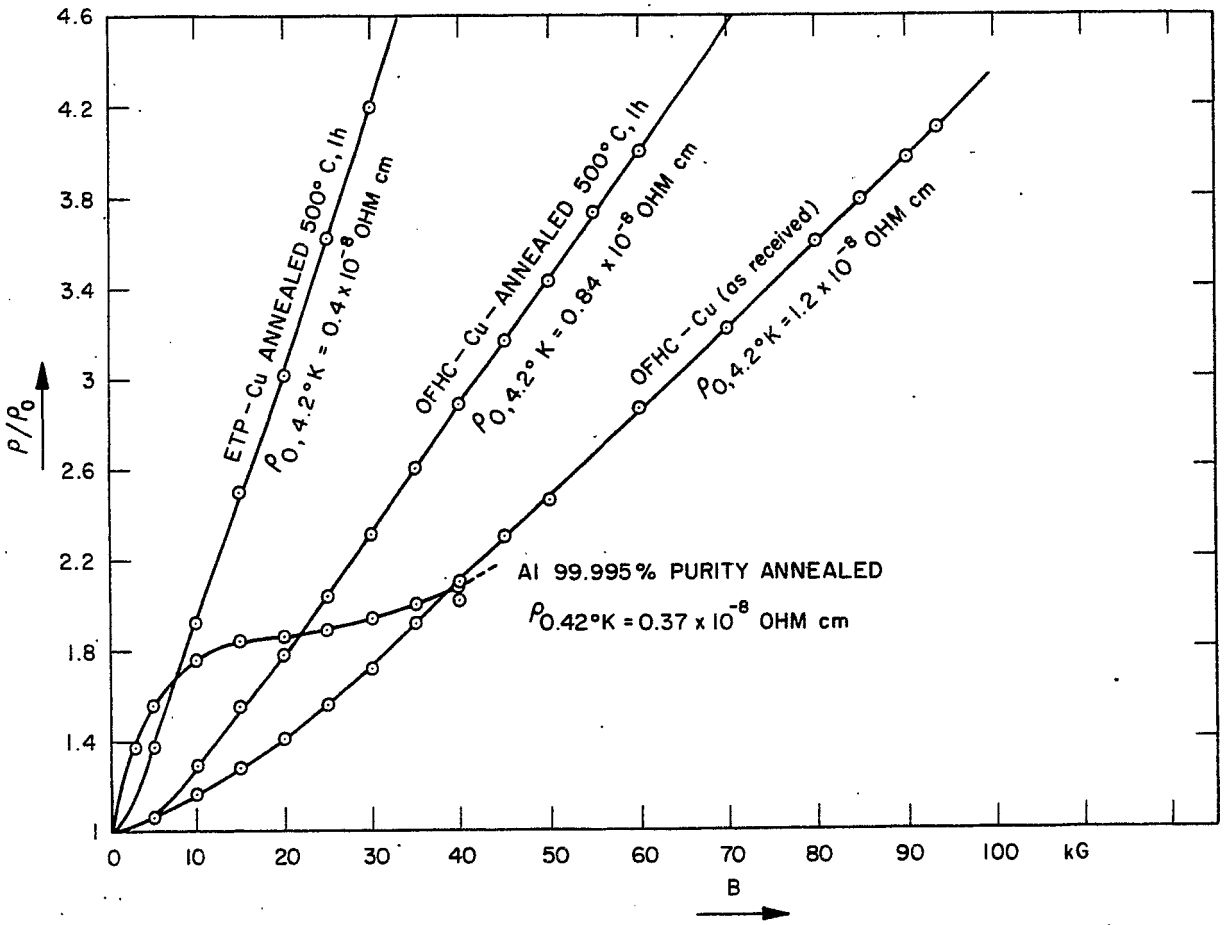

Fig. 3. Magnetoresistivity curves of copper and aluminum. (No mechanical stress.)

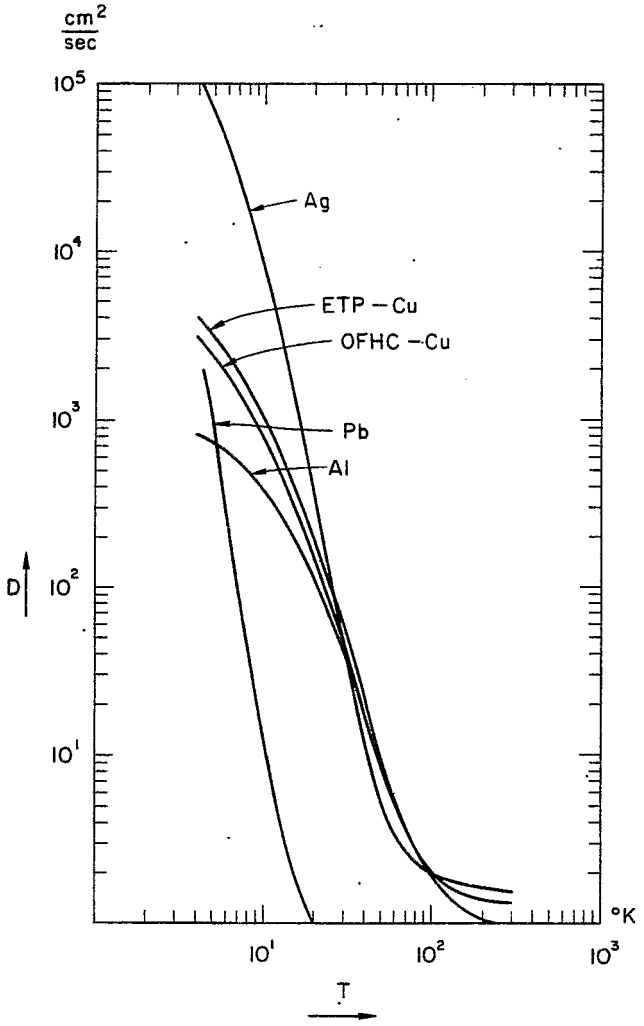

Fig. 4. Thermal diffusivities of a few commercially obtained metals. (No mechanical stress.)

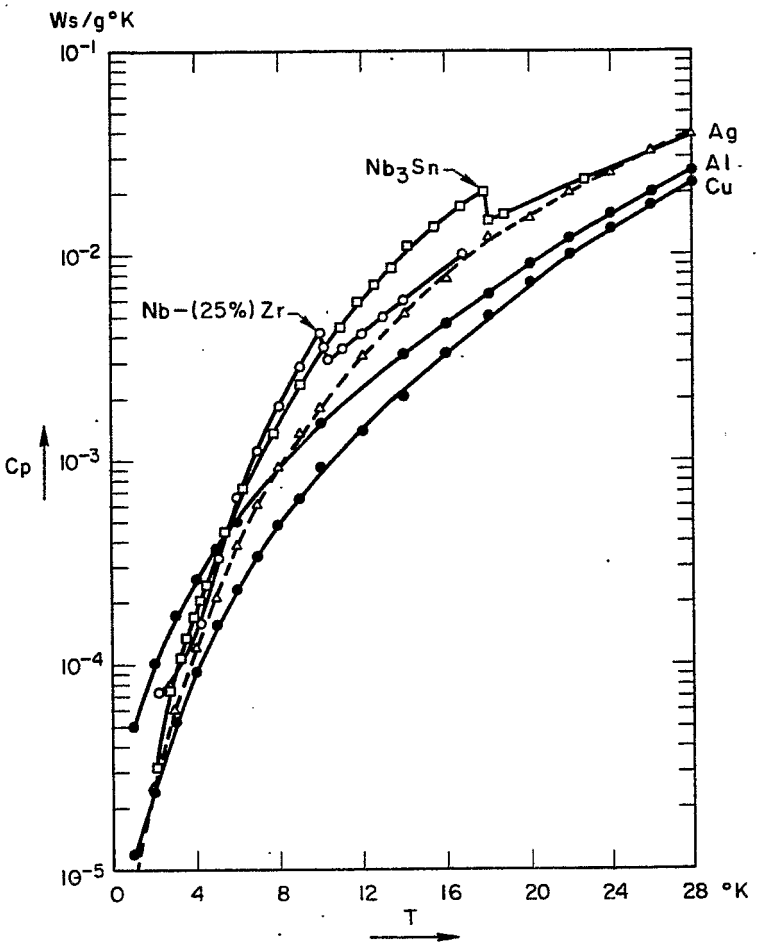

Fig. 5. Specific heat vs temperature for superconducting type II materials and normal metals.

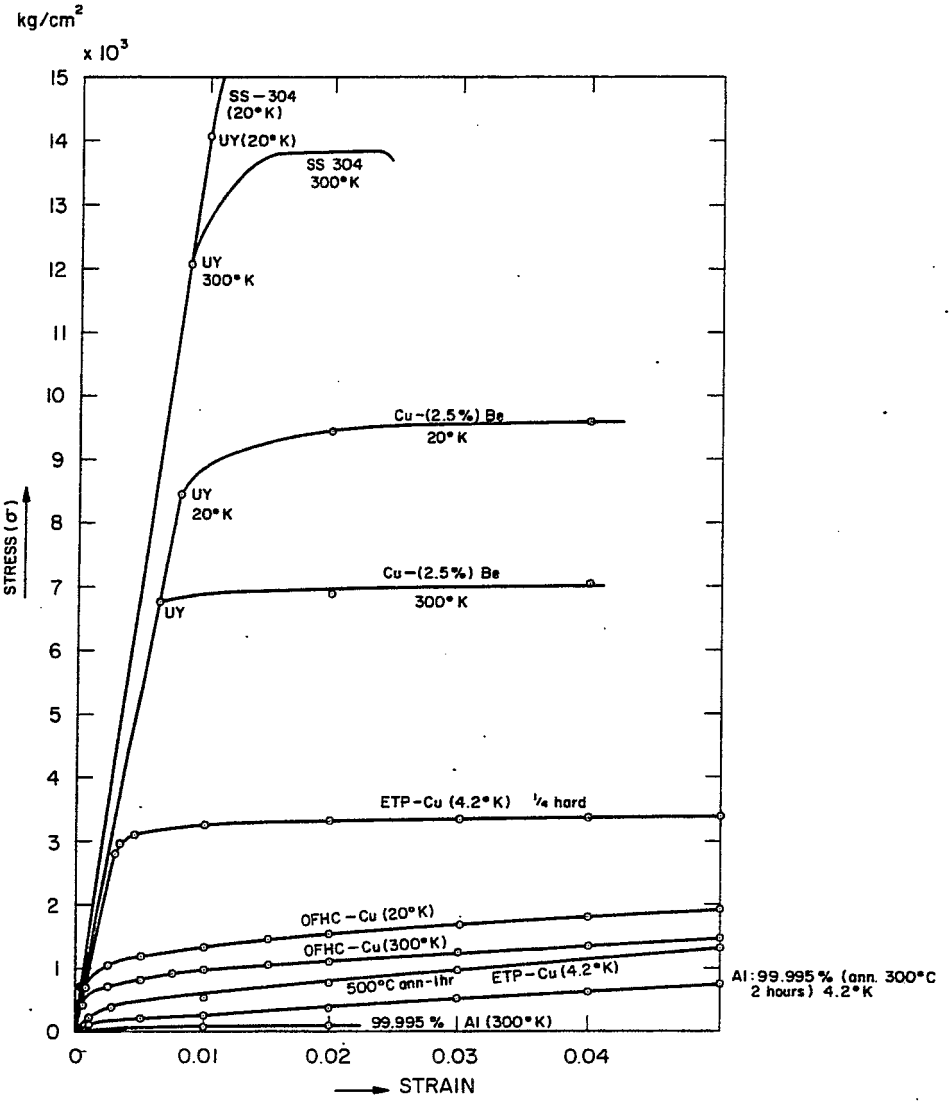

Fig. 6a. Stress-strain diagrams of normal metals.

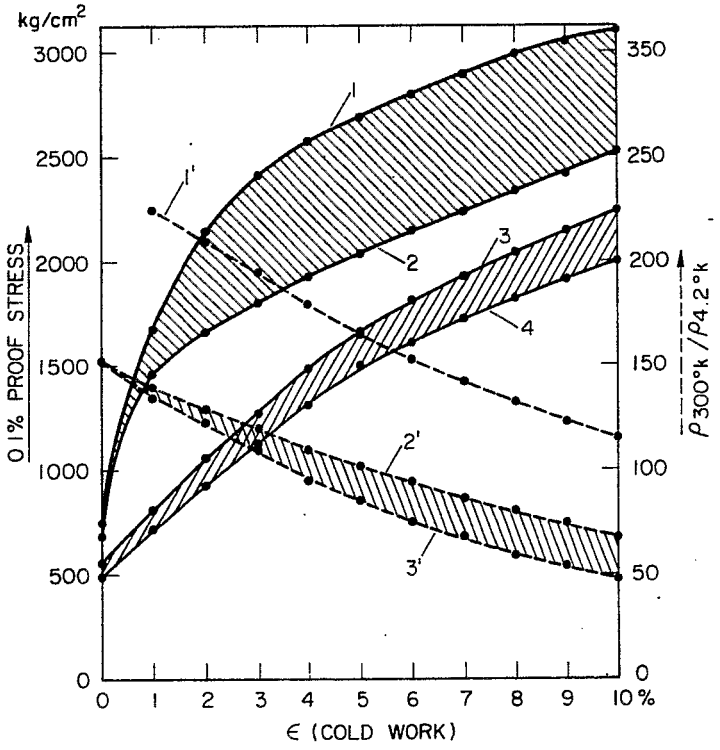

Fig. 6b. Effect of mechanical strain on the performance of copper and composite conductors at 4.2°K:

1. Nb(60%)Ti and Cu, composite conductor: 3 to 1 Cu to SC ratio.
2. Nb(60%)Ti and Cu, composite conductor: 5 to 1 Cu to SC ratio.
3. 99.995% Cu, soft, as received.
4. 99.995% Cu, annealed.

1′. 99.995% annealed copper.

2′. Nb(60%)Ti and Cu, composite conductor: 5 to 1 Cu to SC ratio.

3′. Nb(60%)Ti and Cu, composite conductor: 3 to 1 Cu to SC ratio.

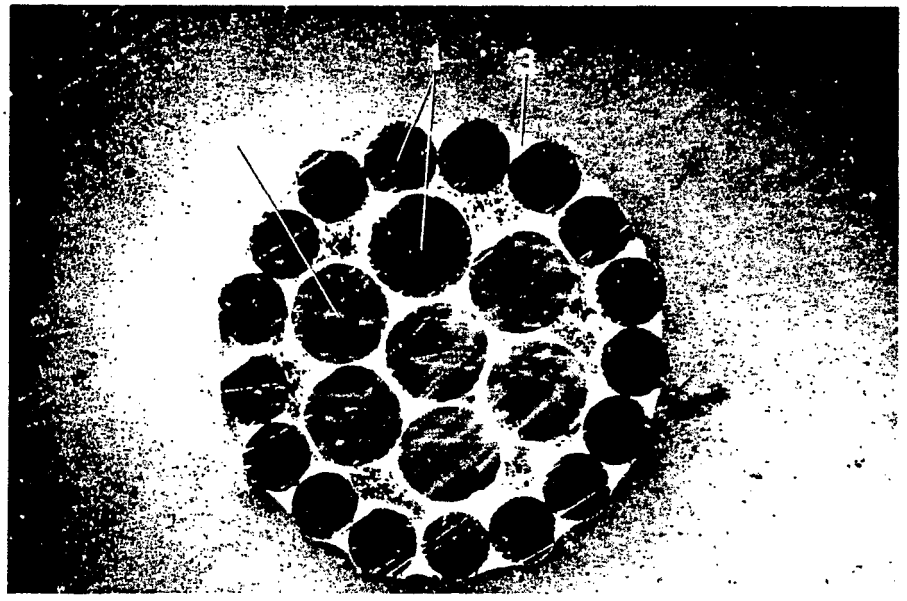

Fig. 7. Nb(22at%)Ti-Cu — cable.
1. Cu — strand.
2. SC — filament.
3. Ag — Sn alloy.

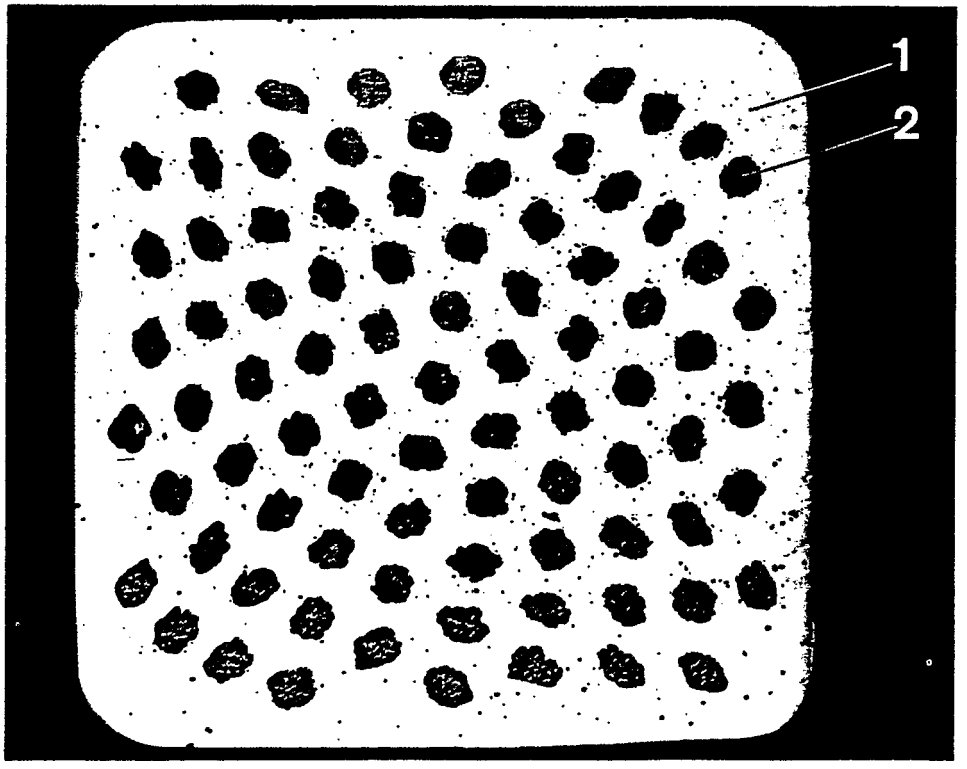

Fig. 8. NbTiCu composite conductor.

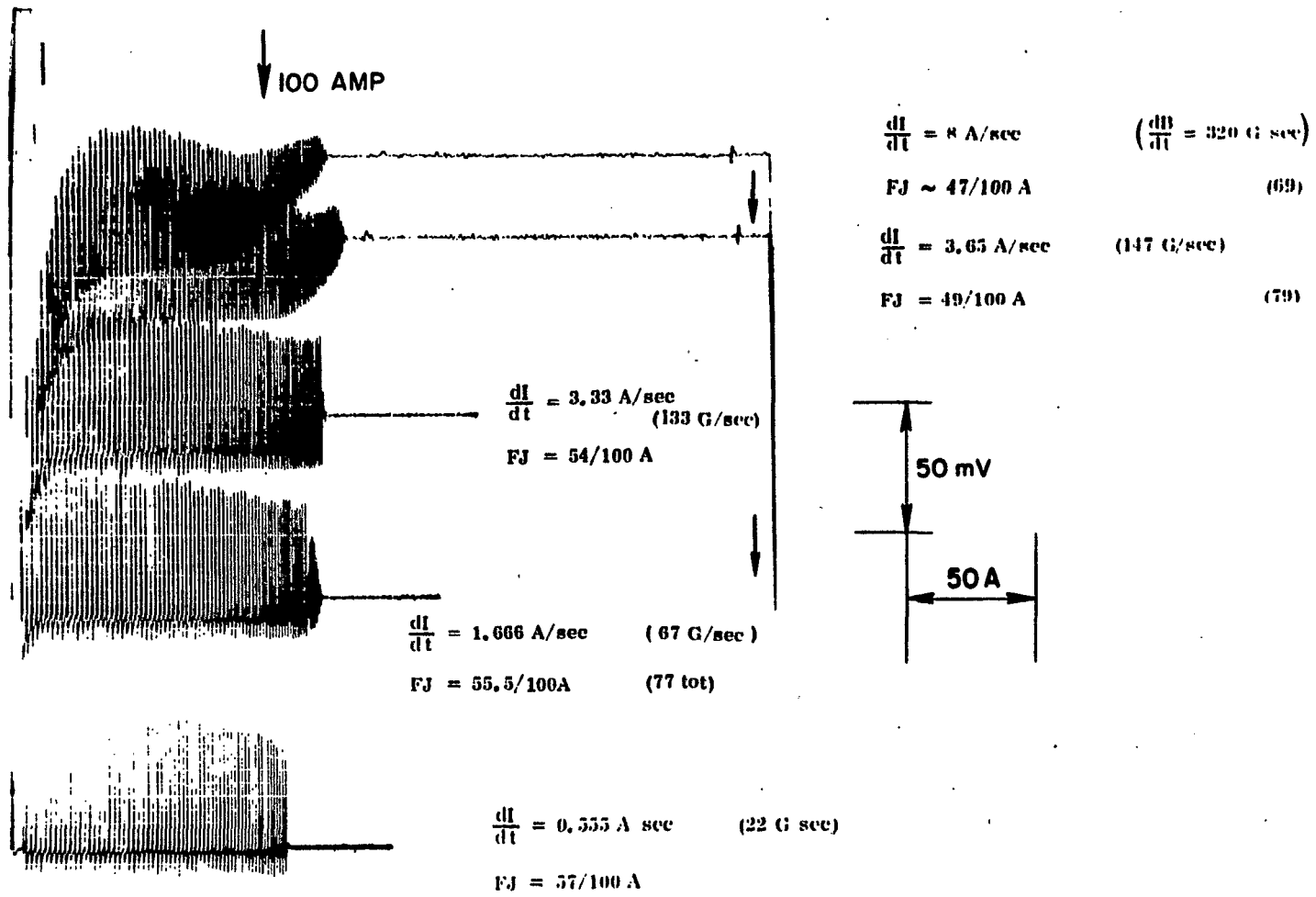

Fig. 9. Voltage current oscillograms of medium size magnets. (The individual turns are insulated by means of a multifilamentary nylon ~ Nomex.)

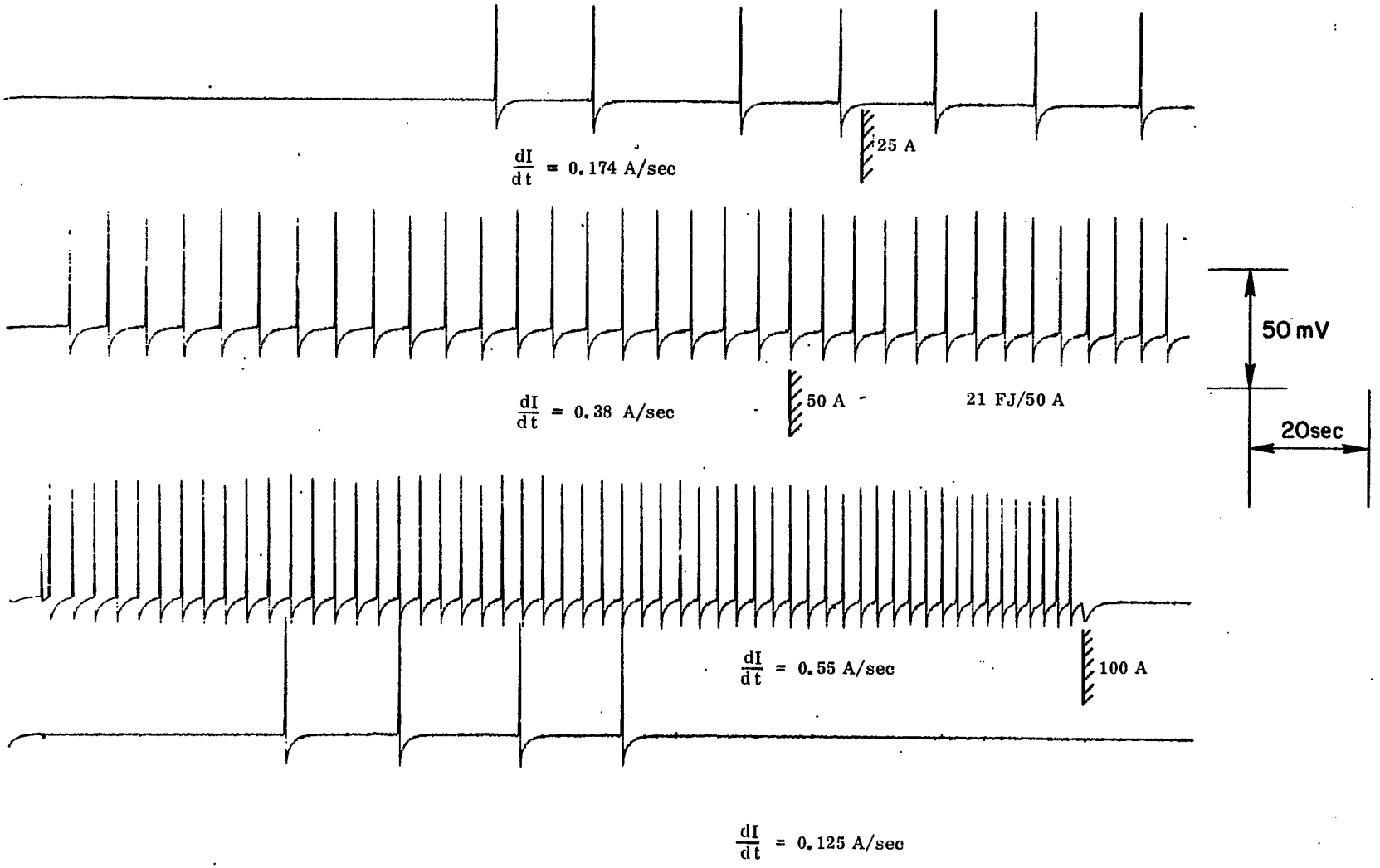

Fig. 10. Flux jump pattern due to internal short circuits in the magnets.

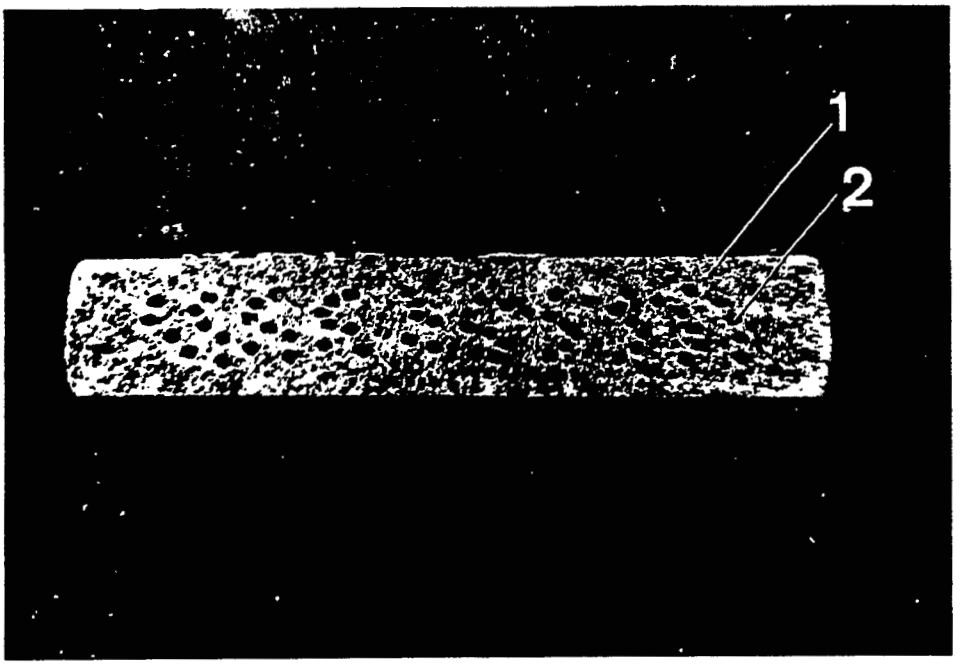

Fig. 11. Nb(60%)Ti-Cu composite strip.

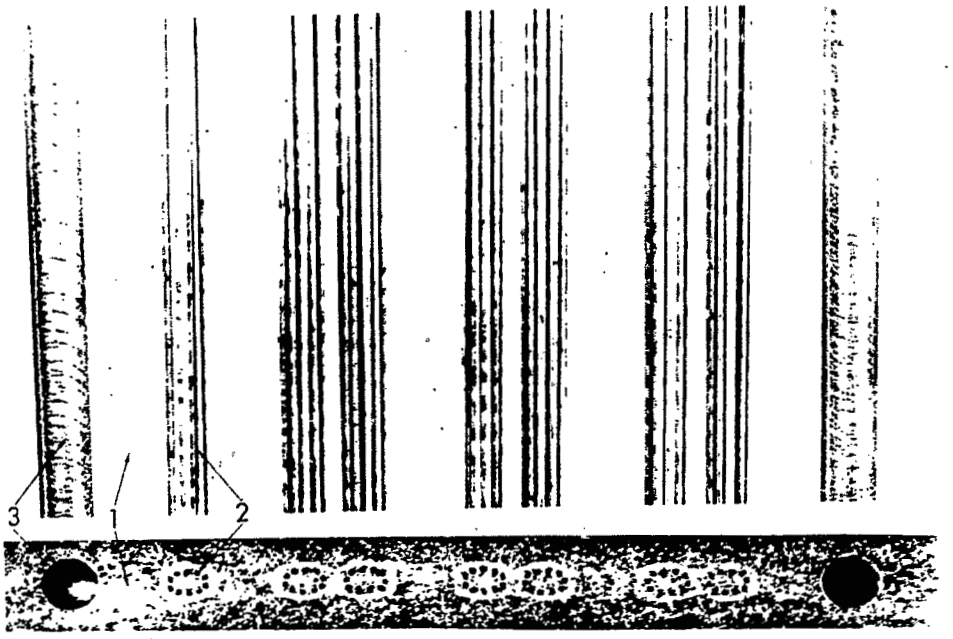

Fig. 12. NbTiCu composite conductor reinforced with stainless-steel wires.
1. Copper substrate.
2. Superconducting filament.
3. Stainless-steel reinforcement.

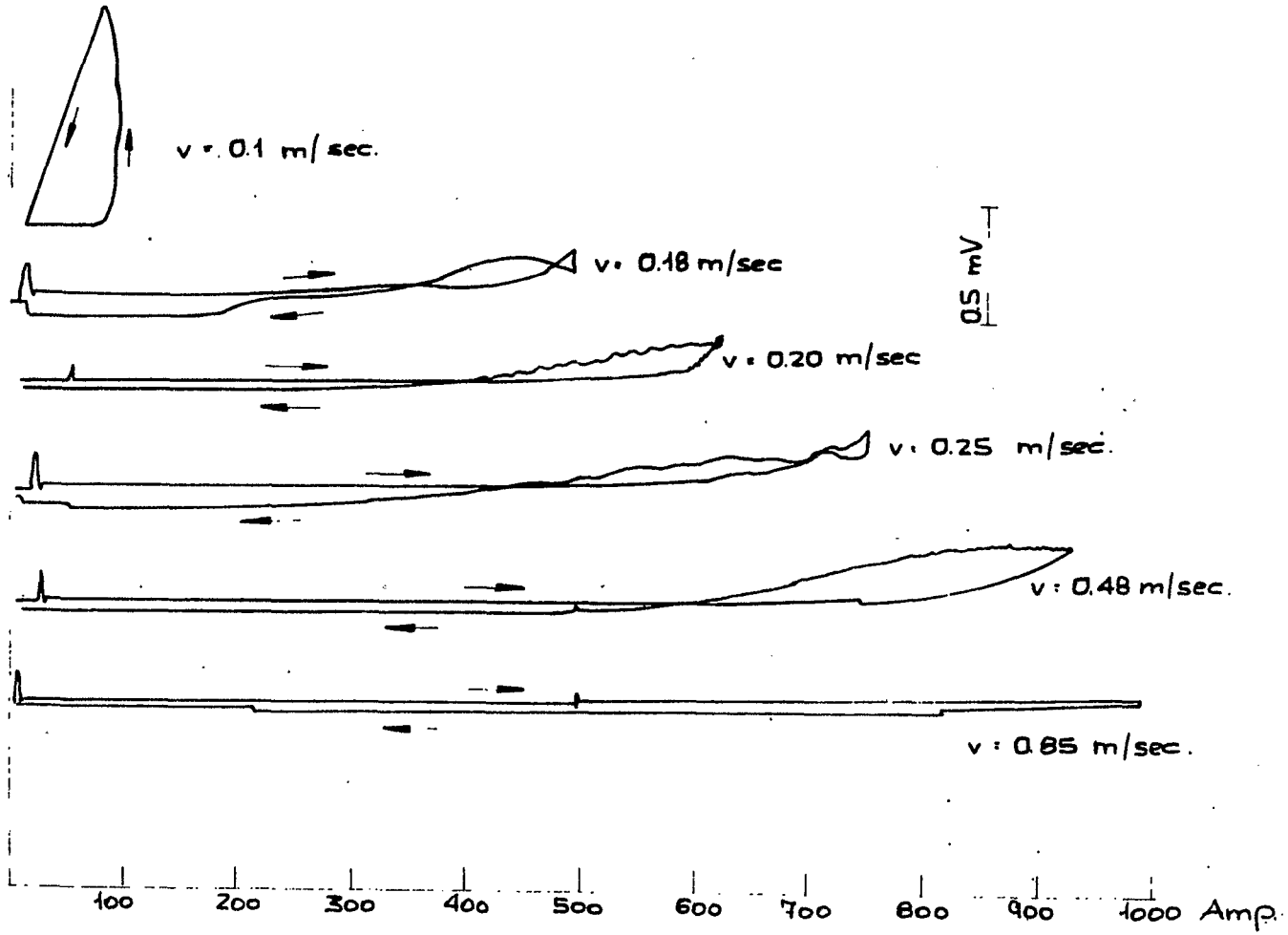

Fig. 13. Current-voltage diagrams measured at various helium flow rates in hollow composite conductor (Nb_3Sn and Cu).

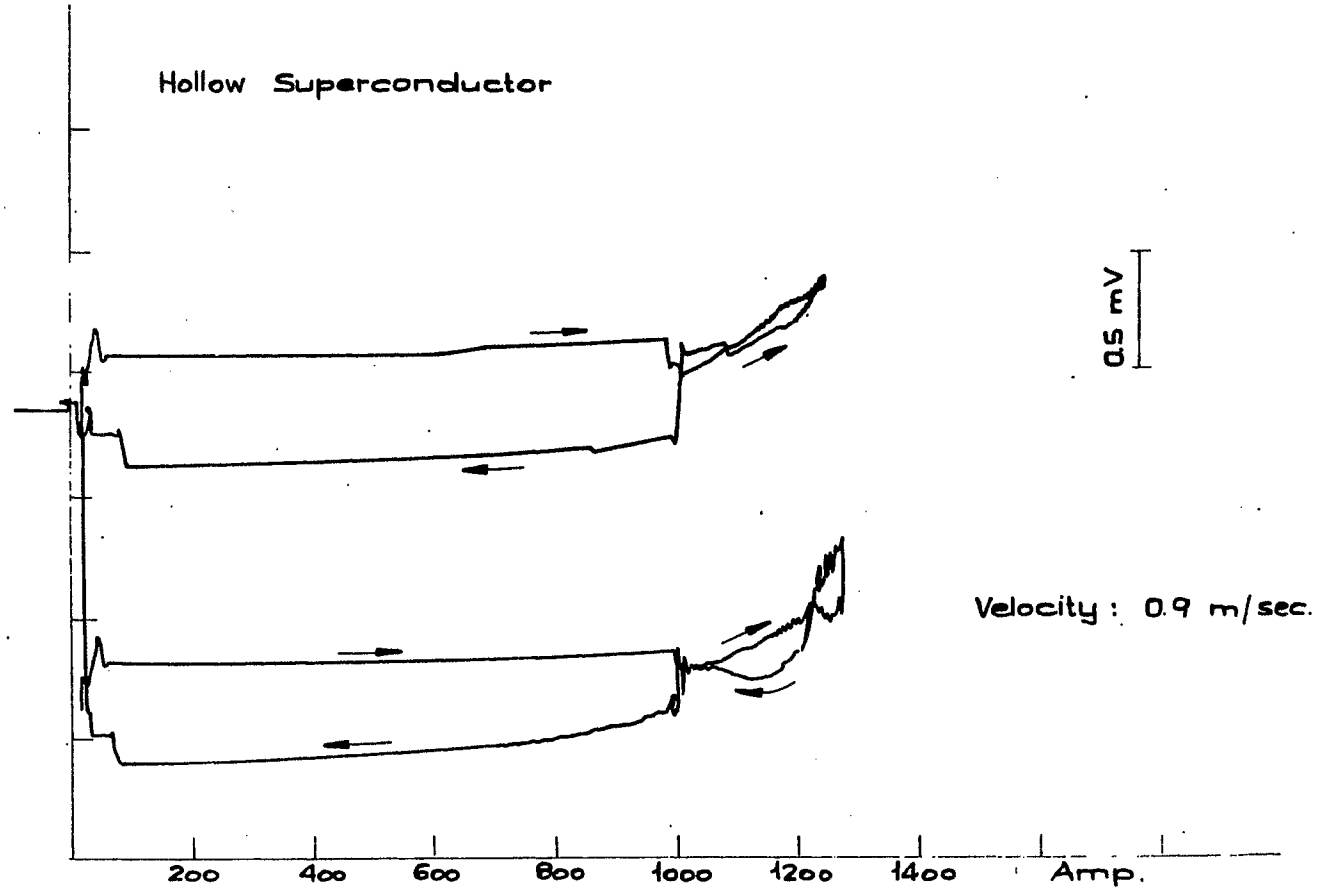

Fig. 14. Voltage-current diagrams in a (Nb_3Sn)-Cu hollow conductor wound into a single layer coil. The length of the hydraulic passage is $\sim$ 3 m.

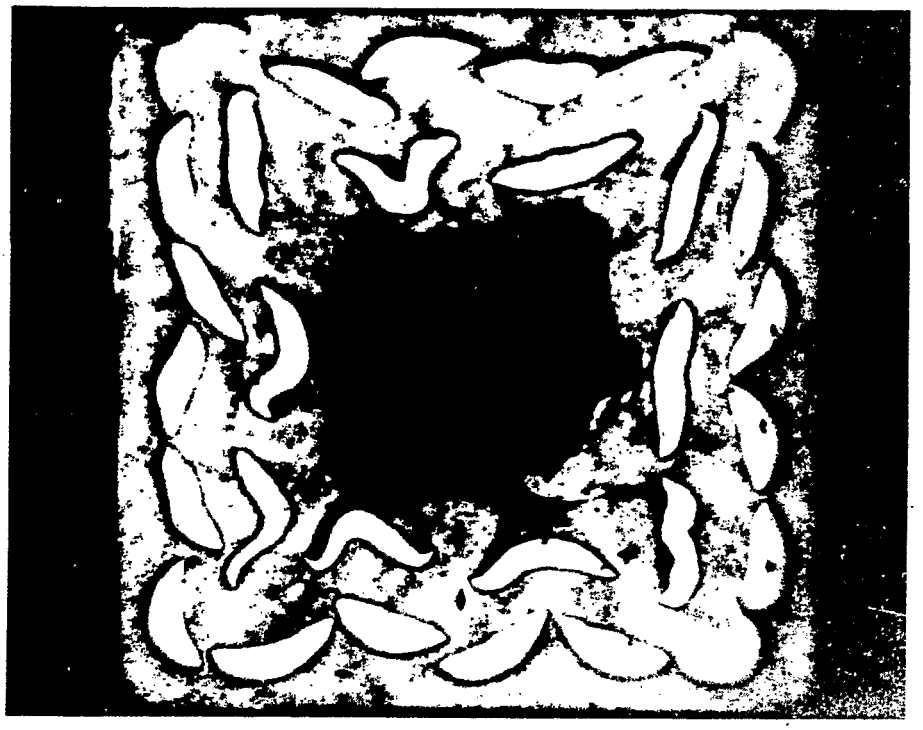

Fig. 15. Nb(60%)Ti-Cu hollow composite conductor, 0.5 x 0.5 cm^2 over-all dimensions, 0.22 x 0.22 cm^2 coolant hole. Although the individual superconductors are severely distorted, the conductor shows short sample performance (Cu:SC ratio 2.8:1).

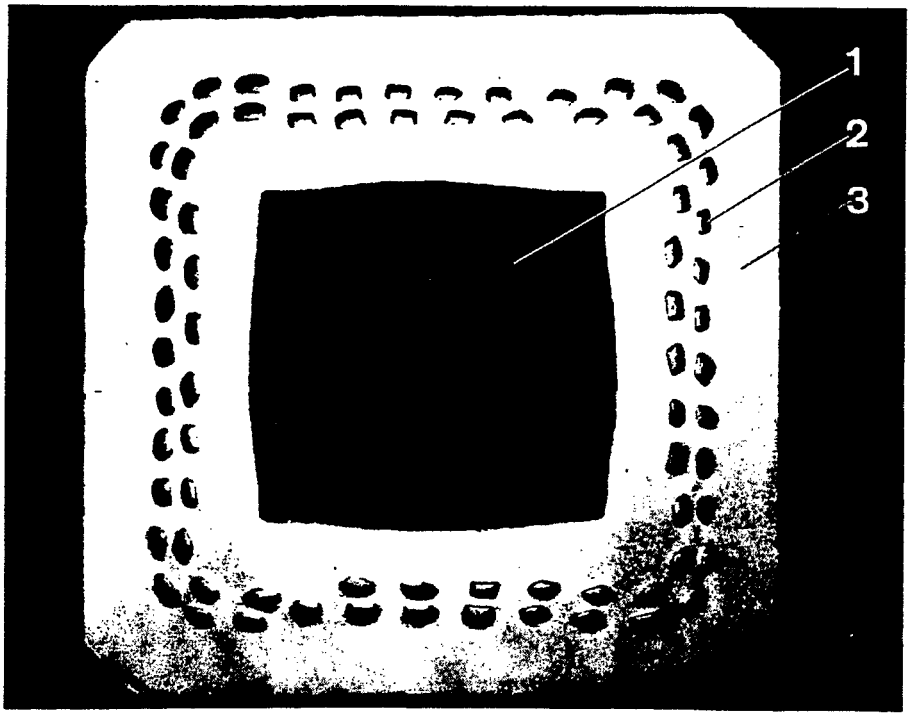

Fig. 16. 5000 A, 60 kG hollow composite conductor. Over-all dimensions 1.2 x 1.2 cm^2.

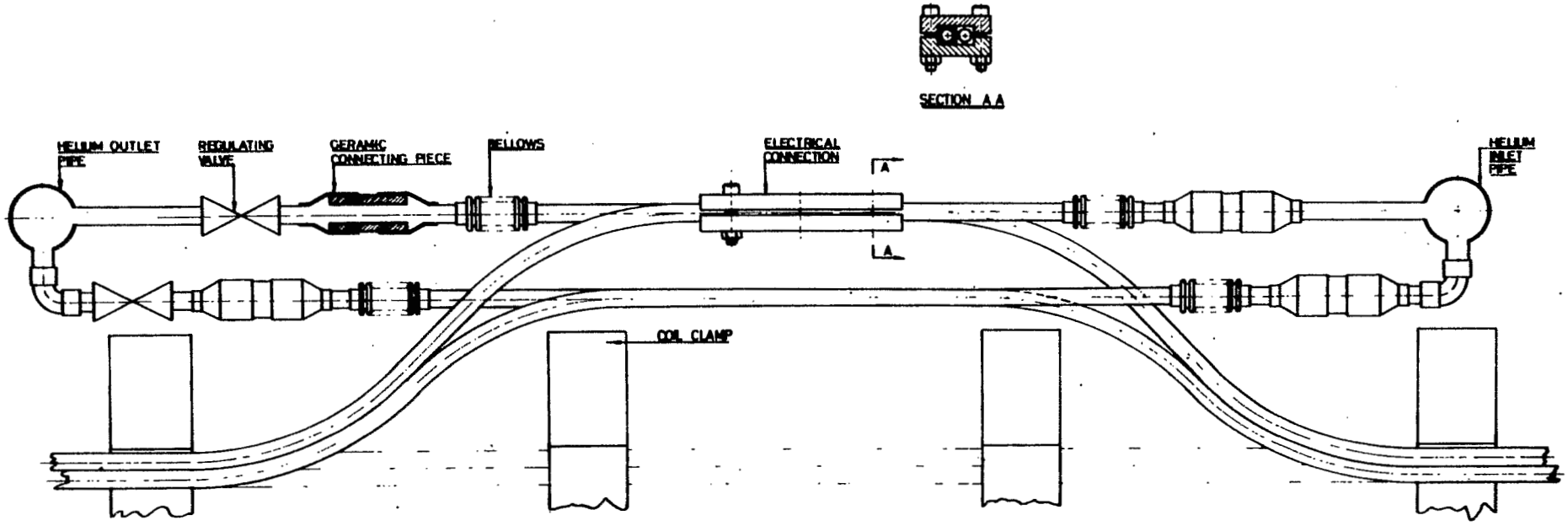

Fig. 17. Proposal to disconnect electrically each hydraulic passage by means of reinforced ceramic tubing.

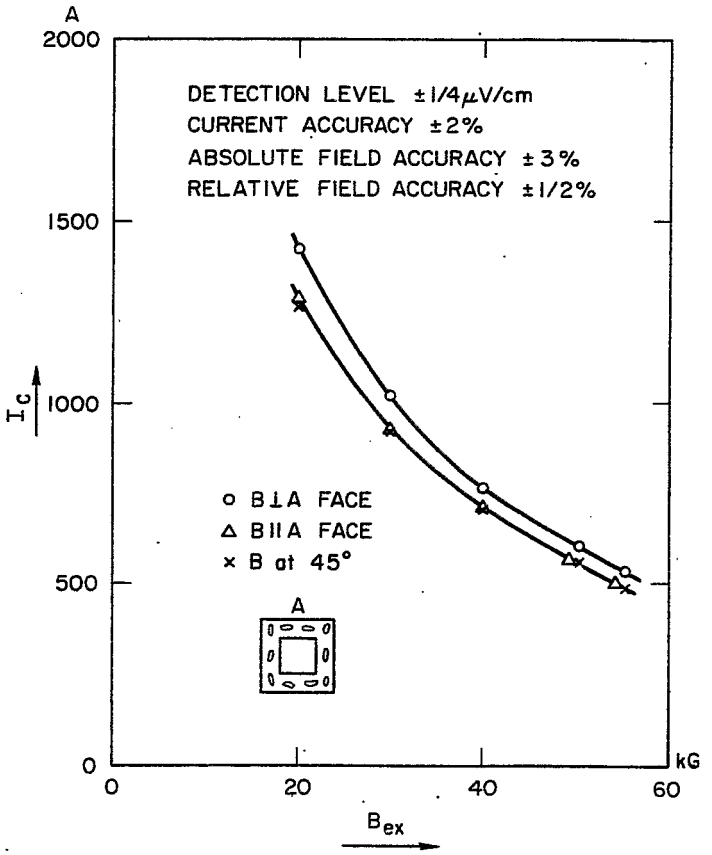

Fig. 18. Anisotropy effect on a hollow composite conductor (courtesy IMI).